Physical processes and modelling at ocean margins

Ramiro Neves[a], Henrique Coelho[b], Rui Taborda[c] and Pedro Pina[d]

a -MARETEC, Instituto Superiror Técnico, Lisbon, Portugal

b - University of Algarve, Faro, Portugal

c - Faculty of Sciences, University of Lisbon, Lisbon, Portugal

d - MARETEC, Instituto Superior Técnico, Lisbon, Portugal

Abstract

Ocean margins are very productive areas and consequently they are interesting both for scientific and socio-economic reasons. Their economical importance was the main reason to support integrated projects to understand and quantify the processes responsible for high biological productivities, in order to create the scientific knowledge required for its management.

For long time it was believed that high productivity of ocean margin areas was a consequence of the discharge of nutrients form the continents. As the scientific knowledge of the processes taking place on those areas increased, it was shown that biological productivity of the ocean margin is mainly a consequence of the complexity of the physical processes taking place on those areas and only in semi-enclosed areas (*e.g.* estuaries) a consequence of continental discharge. This conclusion has enhanced the importance of the development of integrated studies involving fieldwork and modelling.

The complexity of physical problems taking place on ocean margins is a consequence of local depth gradients (e.g., continental slope and submarine canyons), but also of the wide range of forcing mechanisms driving the flow – wind, density and tides. The combination of these forcing mechanisms lead to a even more wide range of phenomena like, upwelling, fronts, internal waves, surface gravity waves, etc.

To understand processes going on, process-oriented models can be used. However the final product for modelling processes in coastal areas must be an integrated model based on the primitive equations for mass and momentum. For management purposes this model has to couple physical and biological processes.

In this paper a general modelling framework is described. This tool is developed to accommodate models for physics, biology and sediment transport. Numerical solutions, processes and results for the Iberian margin and for the Tagus Estuary (Portugal) are described.

Introduction

A typical ocean margin has a continental shelf about 200 m deep, and a steep slope (5 to 10%) down to the abyssal plain with depths of the order of 4 to 5 km. Although the continental shelf is the transition zone from the continent to the deep ocean, this does not mean that biological production on the shelf is directly related to the discharges from the

continent. Exchanges between the shelf and the deep ocean due to the circulation pattern (horizontal and vertical) are the main source of nutrients for shelf areas.

There are several mechanisms that are candidates to promote this exchange. Coastal upwelling typical of subtropical eastern ocean boundaries generates cross slope exchange due to Ekman offshore transport. In the surface layers wind forcing blowing form north together with Coriolis force push surface water offshore, lowering sea level along the coast. This surface depression, together with vertical shear and with coriolis force generate a vertical distribution of velocity that creating a onshore subsurface transport bringing nutrients from the deep ocean into the shelf region, to the photic zone. Associated to coastal upwelling there are equatorward jets that often become unstable via barotropic and/or baroclinic instability generating eddies and filaments that can transport considerable amounts of material across the shelf break. Other typical features of the ocean margins are along shore currents generated by pressure gradients. Some examples are the typical slope currents of the eastern ocean boundaries driven by the meridional pressure gradients and the currents originated by river plumes of fresh water. In both cases, the currents are topographically trapped but in the presence of bottom irregularities such as submarine canyons or capes they can produce cross slope exchange.

Tides acting on a stratified fluid generate internal tides, which are amplified on the slope, which can propagate across the shelf. Internal tides and the shorter internal waves propagating on the shelf generate vertical movement and mixing, bringing nutrients to the surface layers and enhancing primary production.

The importance of surface gravity waves generated by wind depends on the ratio between their height and local depth and on their frequency. Along the coast they are always important, generating coastal currents, which play a crucial role on beach sediment transport. The importance of currents generated by the waves decreases with depth. However even in deep areas they can induce instantaneous high frequency velocities that added to lower local low frequency velocity can create conditions for resuspending bottom sediments, which become available for transportation. This process is essential for geological studies, and is for reoxygenation of the upper layer of bottom sediments, increasing the mineralising rate of bottom organic matter.

Classical ocean models use finite-difference methods and rigid laws to perform vertical discretisation. In finite-difference methods partial differential equations are transformed into algebraic equations replacing derivatives by differences between state variables values calculated at points of a space (or temporal) grid. On a Cartesian reference, the most convenient horizontal grid is rectangular. For large size models the most convenient coordinates are geographical and grid lines coincide with meridians and parallels. Finer grids generate in general the most accurate results.

In ocean systems the horizontal dimension is orders of magnitude larger than vertical one and strong depth gradients can be found, which are generally maximum along the ocean margins. Persistent features of ocean circulation are in general associated density gradients associated to vertical distributions of temperature and salinity. In traditional models the vertical coordinate is chosen according to the importance given to each of those aspects (topography or density). A common drawback of those models is that they can't shift from a coordinate to another.

In sigma coordinates each layer occupies a constant percentage of the water column thickness and the number of layers becomes independent of the local depth. This type of coordinate is adequate when the topography payer the major role in the circulation. In isopycnic coordinates layer are coincident with isopycnic levels (levels of equal density). This coordinate is the most convenient when the flow follows isopycnic levels, which is the case when density is the major forcing mechanism. If topography plays a major role or vertical transport destroys the vertical gradients this coordinate becomes inadequate. Cartesian coordinates do not attribute the major role to any of those mechanisms, being in fact a compromise between different coordinates, in models that do not allow more than one type of coordinates. The some of the most emblematic examples for each category are: the Miami Isopycnic Coordinate Ocean Model – MICOM [1]; the cartesian Modular Ocean Model – MOM [2]; the sigma coordinate model Semi-spectral Primitive Equation ocean circulation Model – SPEM [2]; and the sigma coordinate Princeton Ocean Model – POM [3].

That there is no ideal solution for the vertical coordinate is clear from the results of DYnamics of North Atlantic MOdels - DYNAMO – project [4]. The most satisfactory grid should always be oriented with the flow and so must be a compromise between the various available possibilities, depending on the physical processes that determine the flow in any particular region. Sigma models reveal strong topographically-determined currents, making these models the best choice whenever flow is constrained by depth contours. However, if the flow follows surfaces of constant density, as may be the case near the seasonal thermocline in periods of low turbulence intensity, sigma models can, numerically speaking, erode these surfaces, and in such instances isopycnal models are a better choice, in spite of the numerical difficulties associated with them. The shortcomings of sigma models in stratified regions can be reduced by a slight change in the conceptual formulation. The computational model may be divided vertically into two sigma models, separated by an interface placed at a level of nearly horizontal motion [6], [5]. This is a compromise between cartesian and sigma coordinates, often called *a double sigma coordinate model*. Generalising this concept to number of sigma domains equal to the number of layers, a Cartesian model is achieved.

Finite-volume integral approaches introduced recently give more flexibility to the choice of the vertical coordinate ([6], [7] and [8]). Using finite-volumes equations are solved on their integral form (the rate of accumulation of a property inside a volume is equal to the integral of the fluxes across its boundaries plus the production inside the volume). In this case the vertical discretisation is limited only by the complexity of the integrals involved in the calculation. A great achievement of this method is the possibility of combining different classical discretisations in one simulation (e.g. Cartesian below the thermocline and sigma above).

The choice of the vertical coordinate is essentially a problem for the physics. It is very important to simulate the circulation and is also essential for the simulation of advection-diffusion on biogeochemical models. The vertical coordinate is irrelevant for the simulation of the biochemical reactions involved on marine environment processes, which depend on the local properties of the water only (concentrations, temperature, light, etc.). Most of these processes are site independent, occurring in coastal areas, on the shelf or in the deep areas. The complexity of the biochemical processes requires a

large number of developers, which is easily achieved if a common model is used on all those areas. More than a model, the simulation of the marine environment needs a modelling framework based on a modular approach, where modules are easily coupled.

This paper describes a modelling framework, a circulation module, the turbulence closure, a sediment transport model and some results.

Modelling Framework

The need to understand the processes in the ocean soon conduced to the development of models. The departure point for physicists and for other disciplines was very different. Physicists knew the general equations for fluid dynamics, their problem being the incapacity to solve them without simplifications; other disciplines still had to look for empirical equations.

Before numerical calculation became possible, both physicists and ecologists had to use analytical procedures. Physicists started for developing models considering a subset of processes and simplified boundary conditions. Ecologists developed simple models of the type predator-prey and investigated on the factors affecting the rates of production and destruction of relevant properties. The advent of computers allowed the development of more complex models and an increasing knowledge of the processes going on in the ocean environment.

Actual computers are powerful enough to develop integrated models coupling physics to other disciplines and are available to everyone wishing to develop modelling. This means that a new philosophy of modelling is being created. Modelling is becoming more and more a group task. It is becoming more and more difficult to a single modeller to know all the system features and all the parts of the code. Data to be entered into a model becomes more and more complex as well as the results of the models. Graphical interfaces are becoming essential accessories of models, for managing input/output complexity. Input and output modules also need to be sufficiently intelligent to allow input file to hold only data required for the processes under simulation. As the complexity of models increases the need of a modelling workbench becomes clear.

A modelling workbench must include separated modules for tasks common to several modelling activities. Examples are input and output tools, grid processing tools, advection-diffusion. A graphical interface to enter data and a post-processing tool able to visualize results can save a lot of time to new users of the system. MOHID ([9], [5],[6]) and TELEMAC [10] were developed following this philosophy. After the development of a structured tool, it was very simple to develop a model for ground water flow, replacing the hydrodynamic module solving the shallow water equations by another one solving the Darcy equation.

MOHID was initially developed as a 2D depth integrated hydrodynamical model for tidal flows in coastal areas [9]. This model was afterwards extended to simulate free-surface waves using Boussinesq equations, 3D baroclinic flow [5], sediment transport [11], ecology [12] and lagrangian transport model and was applied in a variety of conditions ([11], [13], [14], [15]). From these applications, the need for a structured code and a

versatile vertical discretisation became obvious. MOHID2000 was the answer found for this problem.

MOHID2000 is programmed using an object-oriented approach. Each task is performed by a different module, which manages its own data and processes. Objects to enter data into the model and to generate the output were developed using standard formats - ASCII for input and HDF (Hierarchical Data Format) for output. Major modules included in the modelling system process are: bathymetry, discretisation, advection-diffusion (Eulerian and Lagrangian), settling/erosion/deposition of particulate matter, discharges and ecology. Graphical interfaces to process input and output were also developed. Such a system is very flexible and allows quick development of models for other purposes. That was the case of a model for groundwater flow obtained replacing the very complex hydrodynamic module by a simpler module solving the Darcy equation. The rationale used to design the module structure was based on individuality and multi-purpose. Individuality is important to allow the system to be developed by a group, making the work of each member of the group as independent as possible. Multi-purpose is important for development and maintenance efficiency. Input, Output, Bathymetry, Advection-Diffusion and Geometry are examples of modules providing basic services to higher-level modules.

Hydrodynamical model

Equations of a baroclinic 3D model assuming hydrostatic pressure and Cartesian coordinates can be written as, ([5]):

$$\frac{\partial u}{\partial t} + u\frac{\partial u}{\partial x} + v\frac{\partial u}{\partial y} + w\frac{\partial u}{\partial z} - fv = -\frac{1}{\rho_r}\frac{\partial p}{\partial x} + \frac{\partial}{\partial x}(A_H\frac{\partial u}{\partial x}) + \frac{\partial}{\partial y}(A_H\frac{\partial u}{\partial y}) + \frac{\partial}{\partial z}(A_V\frac{\partial u}{\partial z})$$

$$\frac{\partial v}{\partial t} + u\frac{\partial v}{\partial x} + v\frac{\partial v}{\partial y} + w\frac{\partial v}{\partial z} + fu = -\frac{1}{\rho_r}\frac{\partial p}{\partial y} + \frac{\partial}{\partial x}(A_H\frac{\partial v}{\partial x}) + \frac{\partial}{\partial y}(A_H\frac{\partial v}{\partial y}) + \frac{\partial}{\partial z}(A_V\frac{\partial v}{\partial z})$$

$$\frac{\partial p}{\partial z} + \rho g = 0$$

$$\frac{\partial u}{\partial x} + \frac{\partial v}{\partial y} + \frac{\partial w}{\partial z} = 0$$

$$\frac{\partial(S)}{\partial t} + \frac{\partial(uS)}{\partial x} + \frac{\partial(vS)}{\partial y} + \frac{\partial(wS)}{\partial z} = \frac{\partial}{\partial x}(K_H\frac{\partial S}{\partial x}) + \frac{\partial}{\partial y}(K_H\frac{\partial S}{\partial y}) + \frac{\partial}{\partial z}(K_V\frac{\partial S}{\partial z})$$

$$\frac{\partial(T)}{\partial t} + \frac{\partial(uT)}{\partial x} + \frac{\partial(vT)}{\partial y} + \frac{\partial(wT)}{\partial z} = \frac{\partial}{\partial x}(K_H\frac{\partial T}{\partial x}) + \frac{\partial}{\partial y}(K_H\frac{\partial T}{\partial y}) + \frac{\partial}{\partial z}(K_V\frac{\partial T}{\partial z})$$

Where u, v and w are the velocity components on space directions x, y and z respectively and p, S and T are the pressure, salinity and temperature. A_H and K_H are horizontal diffusivities and A_V and K_V vertical diffusivities and ρ is the water density related to the temperature and salinity by:

$$\rho = \left(5890 + 38T - 0.375T^2 + 3S\right)/$$

$$\left(1779.5 + 11.25T - 0.0745T^2 - (3.8 + 0.01T)S + 0.698(5890 + 38T - 0.375T^2 + 3S)\right)$$

A prognostic equation for sea surface elevation is obtained by vertical integration of the continuity equation over the entire water column:

$$\frac{\partial \eta}{\partial t} = -\frac{\partial}{\partial x}\int_{-h}^{\eta} u\,dz - \frac{\partial}{\partial y}\int_{-h}^{\eta} v\,dz = -\frac{\partial \overline{U}}{\partial x} - \frac{\partial \overline{V}}{dy}$$

Vertical integration of the hydrostatic pressure equation yields for pressure:

$$p(z) = p_{atm} + g\rho_r(\eta - z) + g\int_z^{\eta} \rho'\,dz \qquad \text{Where } \rho' = \rho - \rho_r$$

This equation relates the pressure at depth z to the atmospheric pressure, the surface level and the vertical integral of density anomaly between that level and free surface. Two first terms are the barotropic and the last one is baroclinic.

The vertical coordinate

The choice of the vertical coordinate is put into different terms for finite-difference and finite-volumes approaches. Finite-difference approaches look for approximations for spatial derivatives, which must be written on a predefined spatial reference. On the contrary, finite-volumes solve integral forms of the conservation principles. In this case fluxes across the faces of a finite-volumes are computed knowing the values on both sides. In this case the shape of the volumes is limited only by the ability to compute the fluxes.

The finite-differences approach

The choice of the vertical coordinate in a circulation model is yet a matter of discussion in the marine modelling community. The ideal mesh should always be oriented with the flow in order to minimise numerical diffusion. The sigma (σ) type coordinates [16] transform the model domain into a constant depth domain and resolve the equations in that transformed domain, allowing the same number of grid points whatever is the local depth being adequate to solve problems where topography plays a major role.

In stratified flows isopycnals are nearly horizontal. Using a σ coordinate, along the shelf break, they are represented by slopping lines that can cross several layers. Another difficulty of the σ coordinates to deal with stratified flows is that the vertical resolution is linked to the local depth and thus can be too poor in areas where density gradients are strong. A double sigma coordinate doesn't completely solve these problems but can minimise them. In this type of coordinates ([5]) the water column is split into two domains and in each of them a σ transformation is applied. The grid used in the upper ocean is linked to the local depth only if the bottom is above the plan splitting the two domains.

Locating the splitting plan under the thermocline, layers in the upper domain - which are nearly horizontal - represent better the flow along isopycnals.

Cartesian and isopycnic coordinates are alternatives to the σ type coordinates. In the former grid lines are horizontal, while in the latter they are coincident with isopycnals. Isopycnic coordinates are suitable to simulate flows where the density plays the major role, while Cartesian coordinates are a compromise between the 3 types, since they are not optimised for any process existing in the ocean. In general they need a big number of vertical layers and can become computationally expensive.

The finite volume approach

The finite-volume approach solves the equations in their integral form:

$$\frac{\partial}{\partial t} \iiint_{CV} \beta dV = - \iint_{surface} \left(\beta \vec{v}.\vec{n} - \nu \left(\vec{\nabla} \beta \right) \cdot \vec{n} \right) dA + S$$

Where β is the volumetric value of the property being calculated, ν is the diffusivity and S represents the sources and sinks of the property. The geometry of the volume is limited for the complexity of the calculation of the surface integral.

Flexible implementations of this approach are got computing distances in the real space (this is not the case of the coordinate transformations in finite-difference methods). Discretisations equivalent to Cartesian, σ or isopícnico coordinates are easily obtained if initial shapes of the volumes are drawn on those grids and if they are deformed following the rules intrinsic to those transformations. Other discretisations can also be used.

The big advantage of the finite-volume approach is that the a unique computer program is used for all the discretisations considered and conveniently organised, different coordinates can be used in different parts of the domain, according to the local conditions. This is the case of MOHID2000. In estuarine applications sigma coordinate is the most used, while in ocean applications Cartesian coordinates are generally more convenient.

The numerical algorithm

The numerical algorithm is independent of the technique used for spatial discretisation. In oceanic areas stability limitations arise mainly from vertical transport and from the propagation of gravity waves. Time splitting methods are the most convenient to handles those limitations. In these methods to perform the calculation in a time step one or more intermediate time levels are considered. A set of processes (e.g. advection/diffusion) modify the property values known at the beginning of the time step and then other processes present in the equation correct these estimated values to conclude time iteration. These methods are generally more stable than the explicit methods and allow the calculation of the different terms of the equation using different numerical schemes.

In MOHID a major goal of the splitting method is to obtain the solution using only tridiagonal matrixes with a time-centred Coriolis term (*fu* and *fv* in hydrodynamic

equations) in order to increase the accuracy of its calculation. Several methods are used in vertical integrated models that can be easily extended to a 3D calculation ([17]). The first method uses 6 finite-difference equations in each time step and others use 4. The former can be more adequate to simulate intertidal areas, but the latter are more efficient in deeper zones if the coriolis term is time-centred. The Coriolis term is a non-derivative term and then its relative importance increases as the size of the modelling area increases.

In MOHID, unknown velocities in the free surface finite-difference equation are eliminated using the corresponding momentum equation leading to tridiagonal matrixes. Knowing the new elevation in each ½ time step the corresponding momentum equation can be resolved with an implicit calculation for vertical transport, inverting again a tridiagonal matrix. In this way the most limiting stability factors: gravity wave propagation and vertical diffusion are resolved implicitly. Courant numbers of 5 are typically used into MOHID applications.

Spatial discretisation is based on Arakawa C grid. In this grid, scalars are computed in the centre of the basic finite-volume, while velocities are computed on their faces. To compute velocities, secondary finite-volumes are defined based on scalar properties volumes. Advective fluxes are calculated considering upstream values. Diffusive fluxes are computed considering central differences referenced to each volume face. For simplicity and accuracy reasons, the pressure is computed using the traditional barotropic and baroclinic components. The baroclinic term is integrated between the level of the velocity being computed and the free surface and the barotropic pressure is computed directly from the surface slope (per unit of volume).

Turbulence Modelling

Previous work, simulating the diurnal cycle of temperature observed during the Long Term Upper Ocean Study (LOTUS) in the Sargasso Sea and the seasonal cycle of temperature off the Iberian coast, showed similar results produced by two different models, based on the [18] one-equation turbulence closure and on the quasi-equilibrium version of the level 2.5 Mellor and Yamada closure scheme [19] respectively. For simplicity, therefore, the one-equation closure scheme was adopted in MOHID2000.

The vertical turbulence fluxes are parameterised using the turbulent viscosity/diffusivity concept:

Viscosity and diffusivities are related to length and velocity scales according to: $K_m = c_k \lambda_k E^{1/2}$ and $K_s = K_h = K_m/P_{rt}$ where c_k is a constant to determined, λ_k is the mixing length, E is the turbulence kinetic energy (TKE), $E = 0.5(u'^2 + v'^2 + w'^2)$, and P_{rt} is the turbulent Prandtl number, assumed to be 1. To close the system TKE is determined from its balance equation:

$$\frac{\partial \overline{E}}{\partial t} = -\frac{\partial}{\partial z}\left(\overline{E'w'} + \frac{\overline{p'w'}}{\rho_o}\right) - \overline{u_H}'w'\frac{\partial \overline{U_H}}{\partial z} + \overline{b'w'} - \epsilon$$

p being the pressure; ϵ is the dissipation rate of TKE; b is the buoyancy, $b = g\,(\rho_o - \rho)/\rho_o$, where g is gravity. The density ρ is determined by a state equation: $\rho = \rho_o[1 - \alpha(T - T_o) + \beta(S - S_o)]$ where 0 refers to a reference state and α, β are respectively the coefficients of thermal expansion and haline contraction. $\overline{X}$ denotes mean quantities and X' denotes fluctuations around the mean.

For the diffusivity of density, $K_\rho = K_m/P_{rt}$. The turbulent diffusivity concept is also used to parameterise the vertical flux of turbulent kinetic energy

$$-\left(\overline{E'w'} + \frac{\overline{p'w'}}{\rho_o}\right) = K_e\frac{\partial \overline{E}}{\partial z}$$

with the usual assumption $K_e = K_m$. The dissipation rate is parameterised as follows: $\epsilon = c_\epsilon E^{3/2}/\lambda_\epsilon$, c_ϵ being a constant to be determined and λ_ϵ the length scale for dissipation.

A difficulty of models that parameterise the turbulent viscosity based on the velocity and length scales is the determination of such scales, especially the length scale. In this model, very simple definitions of the length scales are used, avoiding a large number of coefficients and leading to very reasonable results as were obtained by [29]. The mixing length definitions are $\lambda_k = \min(l_u, l_d)$ and $\lambda_\epsilon = (l_u l_d)^{1/2}$, λ_k and λ_ϵ being the length scales for mixing and dissipation respectively; l_u (upward) and l_d (downward) are obtained from:

$$\frac{g}{\rho_0}\int_z^{z+l_u}[\overline{\rho}(z) - \overline{\rho}(z')]dz' = E(z), \qquad \frac{g}{\rho_0}\int_{z-l_d}^{z}[\overline{\rho}(z) - \overline{\rho}(z')]dz' = E(z)$$

Two constants are to be determined, c_k, c_ϵ. The determination of the constants is part of the model calibration. However, based on laboratory experiments, [20] deduced that $c_\epsilon = 0.7$ is an adequate value for simulations. The choice of c_k is more difficult to justify from observations. Based on the definition of the mixing efficiency coefficient, $\gamma = R_f/(1-R_f)$, where

$$R_f \equiv \overline{b'w'}/(\overline{u'w'}\partial\overline{U_H}/\partial z)$$

is the flux Richardson number, it is possible to deduce that $c_k = 0.15\, c_\epsilon$ (for details see [18]).

To avoid unrealistically small diffusion and dissipation rates in the pycnocline, [18] suggested that a minimal value E_{min} for TKE should be imposed. To match the results of [21] E_{min} is set equal to 10^{-6} $m^2 s^{-2}$. This represents only a simple solution to obtain realistic diffusion rates in the thermocline. ([27] suggested that better results could probably be obtained by parameterising E_{min} as a function of internal wave activity and surface forcing.)

Sediment transport modelling

The continental shelf is a highly dynamic environment, where the flow induced by waves and currents extends to the bottom inducing marine sediment transport. The phenomena of sediment transport in combined wave-current conditions are complex, and not yet fully understood largely to the nonlinear interaction between the flow, bed micromorphology and the moving sediment. Fortunately, substantially progress have been made during the last years concerning the understanding of the all the aforementioned aspects of the problem. Excellent recent reviews are available, including those by [22], [23], [24], [25] and [26].

Two different approaches have been used for predicting sediment transport rate, the so-called energetic method, and the 'process' models. The energetic models, which relate the transport rate to the turbulent energy dissipation (e.g. [27]), are very popular amongst morphological modelers due to their simplicity and ease of use. However, in this type of models the whole physics is incorporated in the coefficient of proportionality between dissipation rate and sediment transport, which can seriously affect their range of application, so they will not be further discussed in this paper.

Process models involve solving transport equations for momentum and sediment concentration subject to appropriate boundary conditions. Differences between these models lies in the assumptions made for eddy viscosity and bottom sediment concentration, which will be discussed in more detail.

Wave-Current Boundary layers

On the continental shelf wind generated waves are generally responsible for the existence of an oscillatory boundary layer of centimetric scale embedded in a much thicker (usually of metric scale) boundary layer of wind-driven or tidal currents. These two boundary layers interact nonlinearly, enhancing both mean and oscillatory bottom shear stresses.

There are numerous models to describe the bottom boundary layer in combined flows. For example, in the scope of MAST G6M Group [28] a list with 21 models have been compiled, and after this date some more have been developed increasing the available list. These models can be divided on five major groups depending on the turbulent closure scheme used: time-invariant eddy viscosity models (e.g. [29], [30], [31]), vertically integrated models (e.g. [32]), mixing length models, one- and two- equation turbulence models (e.g. [33], [34]) and Reynolds stress equation models. In spite of the widely differing formulations, [28] in an intercomparison of eight typical wave-current boundary layer models, showed that the general forms of their prediction of mean and maximum bed shear-stress were broadly similar. These results justifies the use of the simpler models, like the time-invariant eddy viscosity model of [30] and the vertically integrated model of [32], to predict large-scale sediment transport modeling in the continental shelf.

Bed micromorphology

One of the most remarkable features of sediment transport over a non-cohesive sediment bottom is the development of bed geometric shapes in a much larger scale than the

sediment particles in an amazing variety of shapes and patterns. These bedforms have a decisive influence on the structure of the bottom boundary layer, the near bed turbulence and, consequently, on sediment transport. However, in spite of the unquestionable importance or these features, especially in a wave dominated shelf where their presence is almost ubiquitous, their generation mechanism is still poorly understood, as can be seen from the different approximations for predicting their geometry. The most widely used models for predicting ripple geometry in waves are those of [35], [36] and [37]. While the [36] methods tends to strongly over-predict field ripple roughness [38], those of [39] and [37] generally give more realistic results, although the average error is commonly greater than 100% [40].

Under combined waves and currents most authors usually use the wave-ripples predictors solution in a wave-dominated case and a current alone solution for current dominated cases. Recently, [41] have found that this methodology can lead to large errors and have proposed a new ripple predictor for combined flows.

Ongoing investigations, many of which are being carried out in the scope of the EU MAST program, are focusing on better predictions and parameterizations of bed micromorphology.

Sediment Resuspension and transport

Sediment transport within the bottom boundary layer takes place in two modes: suspended load and bed load.

Bedload

Bed load, which involves rolling, sliding and jumping (saltation) of grains along the bed, is the dominant mode of transport for low flow rates and/or large grains. In this mode of transport the particles are supported by intergranular forces as opposed to suspended load where particles are supported by the upward fluid motion.

Several empirical formulas have been proposed to compute bed load transport, being most of them expressed in the form $\Phi = f(\theta, \theta_{cr})$, where Φ is the dimensionless bedload transport rate, θ is the Shields parameter and θ_{cr} the critical value required for sediment movement. One of most used formulas is the Meyer-Peter and Muller, originally developed from data obtained in rivers and channels, given by:

$$\Phi = 8(\theta - \theta_{cr})^{3/2}$$

[42], using a conceptual mechanics-based model for sediment transport processes in steady and unsteady turbulent boundary layer flows, supported the use of a generalized Meyer-Peter and Muller bed load transport relationship for the combined action of waves and currents in the coastal environment.

Suspended load

In a combined flow, sediment is suspended within the wave boundary layer, and diffused further up into the flow by the turbulence associated with the current. Typical wave-current concentration profiles can be divided in two main parts: very close to the bed, in

the wave boundary layer, turbulence is mainly originated by wave oscillatory motion and the concentration profile is similar to the pure wave case, while further up the concentration profile is dominated by current related processes. Following [43] the vertical distribution of time-average suspended sediment under combined waves and currents can be computed by the following Rouse–type equations, were the suspended sediment concentration ($c(z)$) is predicted in terms of the reference concentration (c_R) at elevation (z_R) by:

$$c(z) = c_R \left(\frac{z}{z_R} \right)^{-b_m} \quad for\ z < \delta_{cw}$$

$$c(z) = c_{\delta_w} \left(\frac{z}{\delta_w} \right)^{-b_c} \quad for\ z > \delta_{cw}$$

where b (the Rouse number) is:

$$b_m = \frac{\beta w_s}{\kappa u_{*m}} \quad for\ z < \delta_{cw}$$

$$b_c = \frac{\beta w_s}{\kappa u_{*c}} \quad for\ z > \delta_{cw}$$

u_{*m} and u_{*c} are the maximum and mean shear velocity in wave cycle, respectively, c_{δ_w} is the concentration at the top of the wave boundary layer (δ_w), computed from the first equation, and w_s is the particle-settling velocity. The value of the β coefficient, the ratio of sediment diffusivity to eddy viscosity, is object of some controversy. While some authors argue that in a turbulent flow the particles can not fully follow the turbulent motion, which implies a value less than one, others claim that β should be greater than one due to the centrifugal effects in the eddies. In the literature values between 0.1 and 10 can be found. The observed discrepancies might be related to the attempt to describe all the concentration profiles exclusively by diffusive processes neglecting the convective terms (see [39] and [44] for a discussion). As the behavior of β is still very poorly understood, a value of β = 1 is probably the safest for many purposes [45], thus, assuming that the eddy viscosity and sediment diffusivity can be freely inter-changed.

With the knowledge of the particle-settling velocity the only missing parameter to solve this equation is the reference concentration. In the literature there is a large variety of relationships to compute the reference concentration from the characteristics of flow and sediment properties, being most part of the form [46]:

$$\overline{c}_R \propto \tau'^P \propto u_*'^{2P}$$

where τ' is the skin friction shear stress and μ∗' is the related shear velocity. For the P exponent values between 1 and 15 have been suggested, which express the high uncertainty related with the determination of the near-bottom reference concentration. A major problem concerning the reference concentration is the specification of a reference height. Some authors assumed that the reference level is proportional to the grain diameter ([47], [42]) while others have used a constant height above the bottom [48].

This last approach is generally used in the field experiments due to practical constrains. In the continental shelf scope most authors have used a form of the expression, given by:

$$C_0 = C_b \frac{\gamma_0 \theta'}{1 + \gamma_0 \theta'}$$

where C_b is the volume sediment concentration in the bed, θ' a normalized excess shear stress defined as $(\tau' - \tau_{cr})/\tau_{cr}$ and γ_0 is the resuspension parameter, representing the relative efficiency of sand resuspension. For low values of θ', this expression can be reduce to $C_0 = C_b \gamma_0 \theta'$. The resuspension parameter is somewhat unknown. For example, in a tidal flow over a rippled sand bed [49] found a value of $\gamma_0 = 0.78 \times 10^{-4}$, while the flume experiments of [50] suggested a value of $\gamma_0 = 1.3 \times 10^{-4}$. More recent studies by [51] and [52] conflicts with the previous concept of constant γ_0, indicating that ripple roughness, bed armoring and down-core increase of sediment cohesion can significantly affect the sediment resuspension coefficient. The values of γ_0 from these studies differ more than one order of magnitude, though they both show a systematic decrease in γ_0 with the increase of excess of shear stress. Another source of uncertainty is related with real shelf sediment characteristics. In fact, bottom sediments are generally composed of a mixture of different grain size particles with different compositions, including cohesive fines and are frequently modified by biologic activity, which may deviate considerably the observed values from the theoretical ones. To overcome this problem, a wide suite of tools for monitoring sediment transport in situ has been developed in the last years, which have proven very successful. This new instrumentation has given new insights into sediment transport processes enabling the development of a new generation of process-based models.

Integrated modelling at estuarine scale

The Tagus estuary is one of the widest estuaries in the West Coast of Europe and the larger in Portugal, covering almost a 320-km2 area. The Portuguese capital, Lisbon is the most important city built on its margins.

The metropolitan area has nowadays around 2 million inhabitants, an important harbour and big industrial complexes around the estuary.

The estuary is a mixing place of river and oceanic waters. The salinity distribution depends mostly on the river flow and on the mixing imposed by the tidal regime, which is the main mechanism controlling the distribution of aquatic organisms and suspended particulate matter in the estuary. In ecological terms, it works as a nursery for several species.

Hydrodynamic can be seen as the first driving mechanism of a cascade of complex processes. The water flow is responsible for transporting chemical (e.g. Ammonia), biological (e.g. phytoplankton) and geological (e.g. sediments) in the water column. It is also responsible for the sediments fluxes between the bottom and the water column. The hydrodynamic model was forced only with tide because the main goal is the study of salt marshes and inter-tidal areas where tide is the main forcing mechanism. The cohesive-sediment model use shear stress compute by the hydrodynamic model to quantify bottom fluxes. The sediments concentration deeply interacts with the water quality processes.

The light extinction factor that regulates the amount of light that primary producer receives, is sensible to sediment concentration, causing low production rates in high turbidity areas [12].

Hydrodynamic Processes

Residual velocities presented in Figure 2 (surface values) were obtained through time integration of transient velocities. Residual velocities do not usually provide much direct information but they can be helpful to understand long-term phenomena with time scales much larger than the tidal period. There is a jet outward the estuary associated with a strong anticyclonic eddy off Cascais area; a cyclone and an anticyclone inside the channel reveals a very complex hydrodynamic system coupled with the topography.

This figure shows the Cascais' bay periodic anticyclone (it appears during ebb time) and the outward jet, the maximum velocity occurs in the channel. These features have a strong influence in the bathing coastal area of Cascais; because of this gyre the estuarine ebb water weakly affects the area. Model results (and other field studies) strongly suggest that water quality in this area depends first of all on the proper control of local pollution sources.
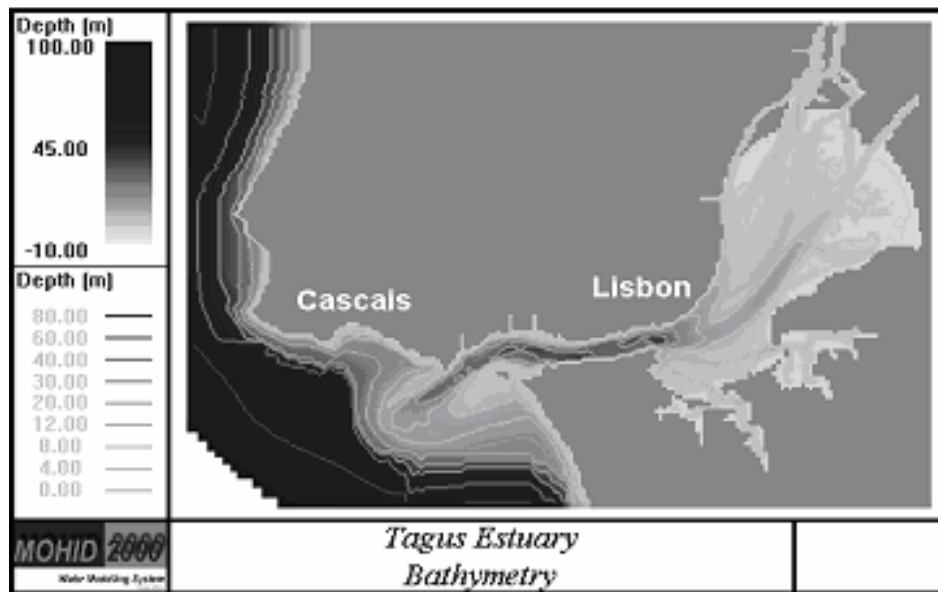
Figure 1 – Tagus bathymetry
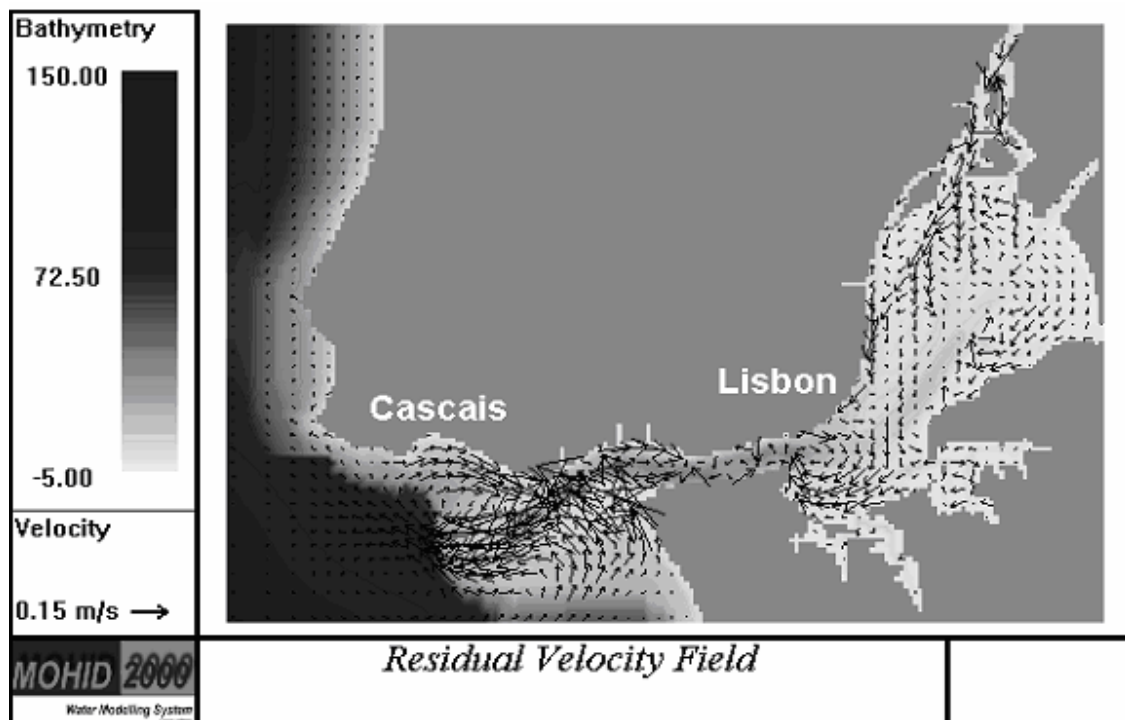
Figure 2 - Tagus Estuary surface residual velocity field.

Cohesive sediments processes

Cohesive sediment transport is simulated solving the 3D-advection-diffusion equation in the same sigma-grid used by the 3D hydrodynamic model using finite volumes for spatial discretization. Horizontal transport is solved explicitly, while vertical transport (including settling) is solved implicitly for numerical stability reasons.

The erosion algorithm is based on the classical approach of [53]. Vertical sediment transport between layers is due to vertical diffusion, vertical advection and sediment settling. The hydrodynamic model computes difusivity and vertical velocity. Settling velocity depends on flocculation processes and is calculated as a function of the concentration [54]. Deposition is modeled as proposed by [55] and modified by [56].

The sediment properties used by the model are those of fine (or cohesive) sediments (particle diameter less than 64 µm), found in the literature for the Tagus estuary. The total mass of suspended sediments can change only due to fluxes across the estuarine boundaries (open boundaries and bottom) and a zero flux condition is used at the free surface. The fluxes across the river boundaries are imposed using field data. In the ocean boundary a constant value is imposed.

Sediment transport plays an important role in water quality. Firstly, the crucial role that suspended sediments impart to the attenuation of the available photosynthetically useful

radiant energy. Secondly, contaminants and nutrients are generally transported along with the sediments upon which they are adsorbed.

Two example cases are presented to illustrate the kind of results obtained: the evaluation of the importance of the seasonal river variability and the potential consequences of sea-level rise. To do so we have computed the difference between a reference situation and the two scenarios.

In what concerns the first case, it must be considered that the river input depends essentially on the policy of management of the river basin. An increase of the agriculture activity, without any modification of the agricultural techniques, increases, in general, soil erosion and, therefore, sediment input to the estuary. Climate changes are expected to increase storm strength and, consequently, erosion. On the contrary, a forestry increase is expected to reduce the sediment discharge.

In Figure 3a one can see strong modifications of the residual fluxes and sediment concentration, mainly in the upper part of the estuary due to a strong reduction of the river input in sediments. These results confirm the observations made by [57] and [58], about the importance of the river input in the dynamical process of sediment transport at the Tagus estuary. Those kinds of results may help the local authorities to better manage the system, at least in what concerns the parameters that depend on the human activity.

The other aspect presented is the effect of the sea level rise. This problem is being object of a great concern mainly along the last decade. Accordingly to most climate change models, a rise of mean sea level is expected in the future. Some predictions point to differences of one meter in certain locations. This value is probably too pessimistic, but it was chosen for our simulation. Being an extreme value it also gives a clear insight of its importance.

Results show that the effects in the estuary will be different according to the regions but, for instance, one of the consequences will be an increase of the erosion processes with direct impacts in the salt marshes areas (e.g. Figure 3b).
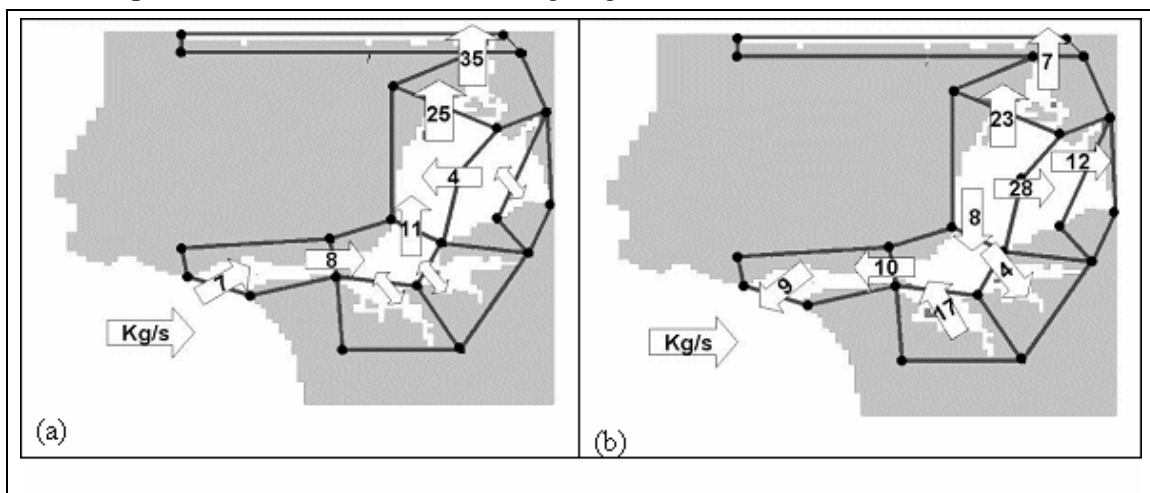
Figure 3: Residual sediment fluxes. Differences between the reference situation and a situation with no river input (a) and a scenario considering a sea level rise of 1 m (b)

Water Quality processes

The Water Quality module has been developed in terms of sinks and sources. Such an approach is convenient to give these models the desired flexibility, providing it with the capability of being coupled to either a Lagrangian or an Eulerian resolution method. Because of the properties interdependency a linear equation system is computed for each control volume and this system can be compute forward or backward in time.

The simulation of the water quality processes is developed with the following considerations. Autotrophic producers consume inorganic nutrients and depend on both their availability and sunlight as a source of energy for photosynthesis. Nitrate and ammonia are the inorganic nitrogen forms that primary producers consume. The Primary and Secondary producer's excretions are considered, acting as source for the nitrogen cycle. Primary producers are consumed by secondary producers, which in turn are consumed by higher trophic levels.

The following results show time series comparisons between model and field data from the Tagus Field Station 3.5 (Figure 4) [59], for four consecutive years: 1980, 1981, 1982 e 1983

Figure 4 - Field station 3.5 location in the
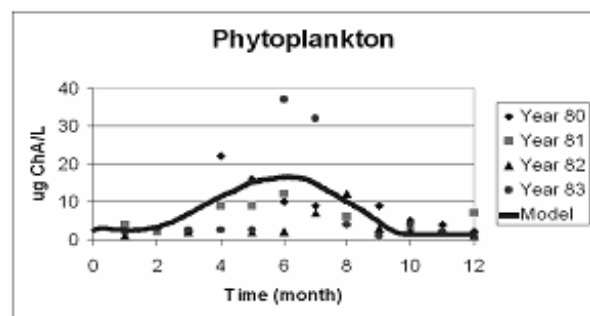
Tagus estuary

Figure 5 - Phytoplankton variation over a year
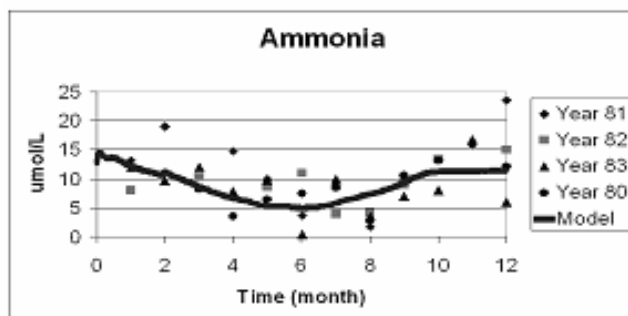
Figure 6 - Ammonia variation over a year
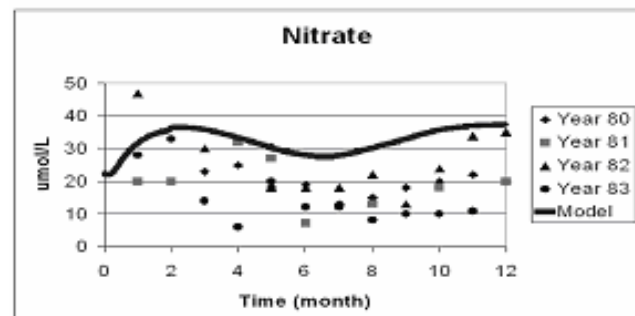
Figure 7 - Nitrate variation over a year
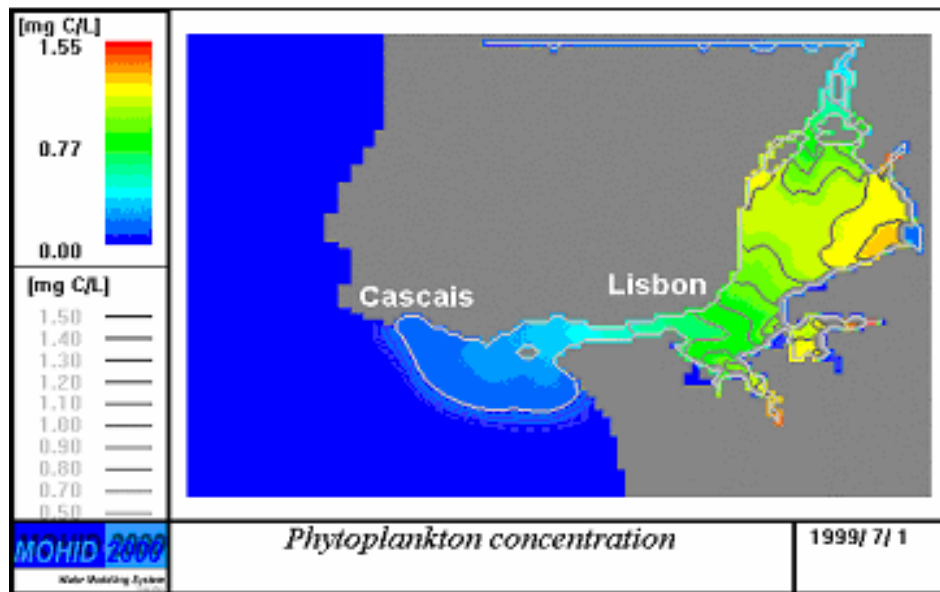
Figure 8 – Phytoplankton distribution at the Tagus Estuary.
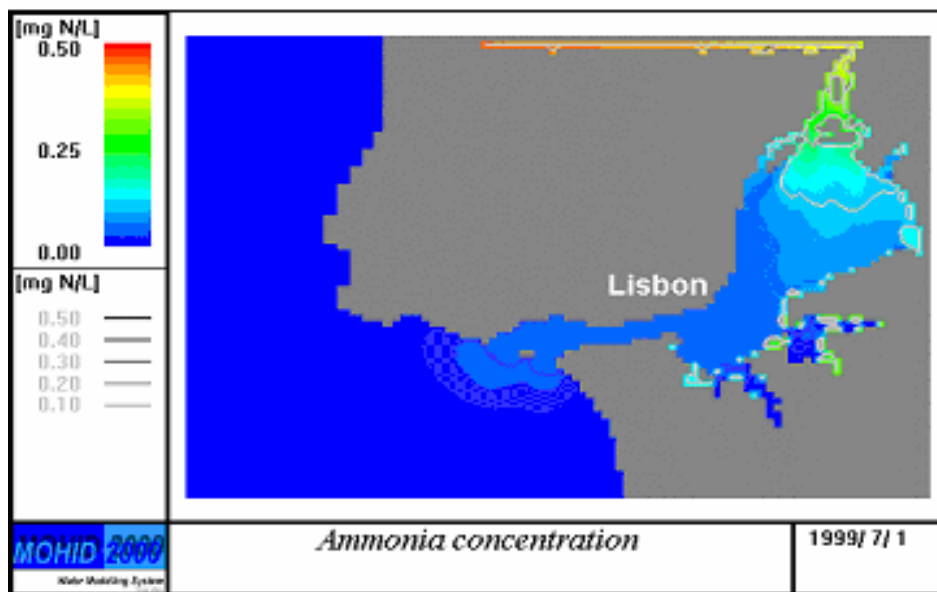
Figure 9 – Ammonia distribution at the Tagus Estuary.
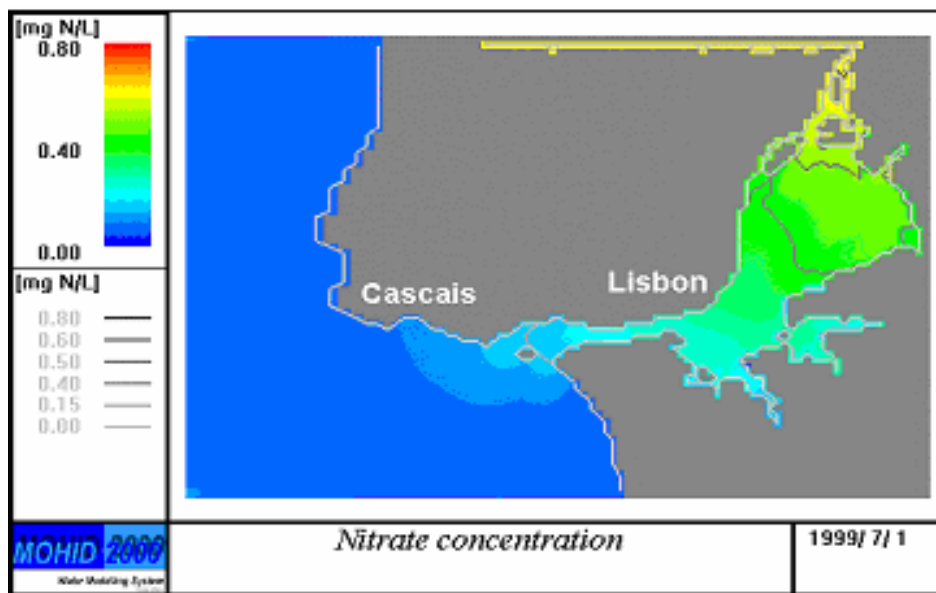
Figure 10 – Nitrate distribution at the Tagus Estuary.

The model results show a higher phytoplankton production in June (Figure 5), caused by the nutrients availability and increased sun radiation. After the bloom the phytoplankton concentration is controlled essentially by the zooplankton strong growth (not represented).Nitrate (Figure 7) and Ammonia (Figure 6) are consumed during the phytoplankton peak, afterwards Ammonia increases due to zoo and phytoplankton respiration and excretion loses and Nitrate increases duo to nitrification processes.

The next results show the spatial distribution of Phytoplankton, Nitrate and Ammonia during the summer period (7, June 1999).

Figure 8 shows a high concentration of phytoplankton in the upper part of the estuary especially in the salt marsh region. Due to the low water level (more light available) and high nutrient concentration this region will have an intense production. The assimilation by phytoplankton preferably towards ammonia causes a strong depletion of nitrogen especially in the higher production areas (Figure 9 and Figure 10).

The next pictures show the time and spatial integrated fluxes of phytoplankton, nitrate and ammonia over a year in the Tagus estuary. In every case the estuary is exporting to

Residual Phytoplankton transport in the Tagus Estuary
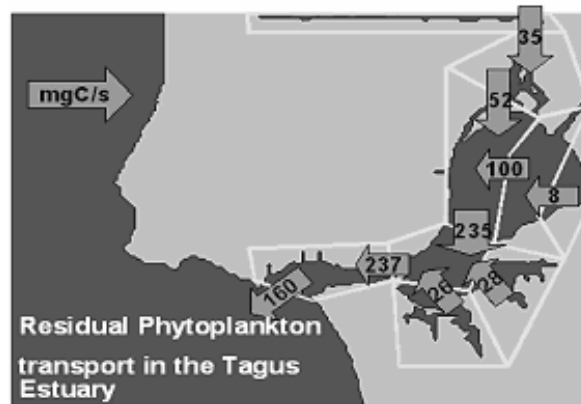
the ocean. The phytoplankton fluxes (

Figure 11) show small river input, all the production occur inside the estuary and afterwards is exported to the ocean. The ammonia fluxes (

Residual Ammonia transport in the Tagus Estuary

Figure 12) show the estuary exporting less then it receives from river input. This can be explained by the fact of respiration and excretion loses being smaller then consumption by phytoplankton. With nitrate (Figure 13) the estuary exports to the ocean more then it receives from the river input. This means that the source term of nitrate, nitrification, is higher then the sink terms, denitrification and assimilation by phytoplankton. These results are influenced by the fact that the pelagic mineralization process was increased because bentic mineralization was neglected for simplicity. This fact gives an unrealistic mobility to remineralized nitrogen that could explain a higher output flux of nitrate.

Circulation in the Iberian margin

Many authors have provided evidence for a poleward flow along West European slopes ([60], [61], [62], [63], [64] and [65]).

Very similar poleward flows have been described in other eastern boundary regions such as the California Current System [66] and the Leeuwin current at the West Coast of Australia. These flows, mainly concentrated along the upper continental slope and outer

continental shelf, appear as undercurrents in the upwelling season and sometimes as surface currents in the non-upwelling season. Some authors suggested that the poleward flow is continuous along the entire eastern boundary and attributed a key role in the transport of Mediterranean water ultimately into the Norwegian sea to the Iberian poleward flow.

[63] described a flow 200 meters deep with geostrophic velocities ranging from 0.2 to 0.3 m s^{-1} and associated transports varying from 300 x 10^3 m^3 s^{-1} at about 38 N to 500 – 700 x 10^3 m^3 s^{-1} at about 41 N. They concluded that the poleward current off the Iberian Peninsula runs for about 1500 km along the upper continental slope of western Portugal
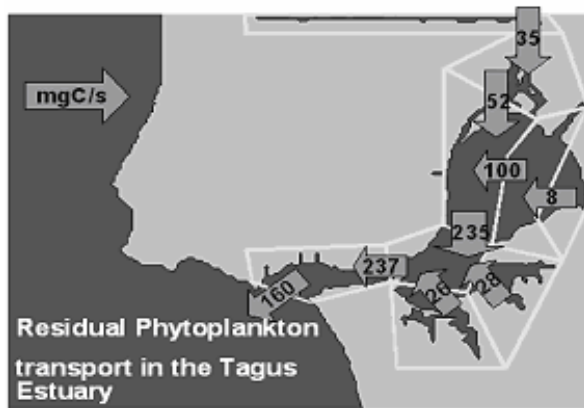
Figure 11 – Residual phytoplankton transport

Figure 12 – Residual ammonia transport.
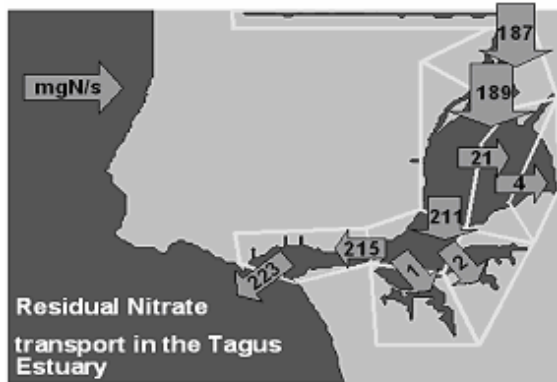
Figure 13 – Residual nitrate transport.

, north-west Spain, northern France and south-west France and that it is about 25 to 40 km wide. (Other reports suggest that the current extends from 1600 m deep to the bottom of the surface layer during the upwelling season and to the surface during the non-upwelling season.) [65] and [67] summarised currentmeter data collected from the Bay of Biscay and presented a residual circulation pattern. Further mention of their work can be found in the section where the model results are discussed. During the last twenty years, several driving models to explain slope currents have been put forward. Of these, the most-frequently-studied have been wind-stress [61], wind-stress curl [68] and thermohaline forcing ([69], [64], [63], [66], [70] and [71]). In fact, off the Iberian coast, onshore Ekman convergence induced by south-south-westerly winds forces a poleward surface flow. The shelfward transport induced by these winds causes a rising of sea level near the coast. The geostrophic adjustment to this sea level distribution will then generate a poleward current. In this case, the longshore acceleration is given by $\partial V/\partial t = \tau_y/\rho H$, where H is the depth of the frictional layer, V the longshore velocity averaged over the depth H, τ_y the

meridional component of wind-stress and ρ the seawater density. Using τ =0.03 Nm^{-2}, ρ =1027 kgm^{-3} and H=200 m, [63] found a longshore acceleration of 0.013 ms^{-1} d^{-1}, which gives V=0.4 ms^{-1} after 30 days. However , the authors argued that other effects, particularly friction, retarded the flow. Assuming a steady state, reached when the bottom stress balances the wind stress ($C_d V^2 = \tau^y / \rho$, being C_d the bottom drag coefficient taken equal to 0.001), they obtained $V \cong 0.17$ms^{-1} which is in agreement with observations. This current should decay seaward from the shelf break and the associated spatial scale is the internal radius of deformation ($\cong$15 km off Iberia). This is what is generally observed both from satellite images and from *in situ* observations. Evaluation of the Ekman volume transports based on windstress measured at Cabo Carvoeiro (west of the Portuguese Coast, 39° N) revealed that only 1/5 of the estimated transport could be explained by the wind, which could not therefore be regarded as the main mechanism driving the poleward current. On the other hand, estimates of large-scale geostrophic eastward transport gives 1.0 m^{2}s^{-1} per meter of meridional coastline. A value of the same order as that estimated from hydrographic sections can be calculated by integrating along the western Iberian coast and adding wind-driven transport. The poleward cooling of the sea surface leads to a meridional increase of surface density causing the dynamic height to drop towards the pole. The large scale eastward flow is generated by this meridional pressure gradient and occurs in the upper 200-300 m. Near the eastern ocean boundary, this flow forces coastal downwelling and a surface poleward current, as confirmed by model results obtained by [70] and [71] for the Leeuwin Current. [69] showed that a combination of shelf-slope bathymetry with a northward density gradient provides a local mechanism that can drive a current towards the pole, as can be expressed by the relation $\rho \, \partial\eta / \partial y = -h \partial\rho / \partial y$ where η is the sea surface elevation and h the water depth (see also [65]). This relation states that sea level decline is proportional to depth h. Therefore sea level declines faster in deep water than in shallow water, so implying a cross-slope sea level gradient. The existence of this gradient leads to a poleward flow over the slope. The cross-slope sea level gradient increases northward and so consequently does the along-slope transport, but this is not a situation that can continue, since friction acts to balance the forcing mechanism [67]. [69] also showed that if the cross-shelf density diffusion is large, the along-slope current is given by $v = \dfrac{1}{2} \dfrac{g}{\rho} \dfrac{\partial\rho}{\partial y} \dfrac{H}{k} h\left(1 - \dfrac{h}{H}\right)$, where H is the oceanic thermal depth and k the bottom friction coefficient. According to this equation maximum velocity must be expected over the slope.

The model domain encompasses the west coasts of Iberia and Morocco, extending from 32°N to 46°N and from 6° to 16°W. The horizontal grid spacing is 8.5 km in both directions. Bottom topography was derived from ETOPO5 by means of an interpolation for the model grid followed by a smoothing using a five point laplacian filter. The bottom depth is then determined, using shaved cells [72]. The model uses 18 vertical layers centred at constant z-levels at depths of 5,20, 45, 80, 130, 200, 290, 400, 530, 680, 850, 1040, 1250, 1480, 1750, 2200, 3000, 4250 m. The western, southern and northern boundaries are open while the eastern boundary is open only at the Strait of Gibraltar.

Lateral heat and momentum diffusion coefficients are 50 and 300 m^2s^{-1}, respectively. On the open boundaries we use the previously referred conditions except at the strait of Gibraltar where salinity, temperature and transports are imposed.

The model is initialised with climatological temperature and salinity fields, horizontal sea level and zero velocity. The climatological temperature and salinity fields are extracted from [73] and [74] and are interpolated to the model grid and then smoothed using a simple cubic spline algorithm. In the upper 500 m, objectively analysed mean monthly Temperature and Salinity fields were used, estimated from CTD/XBT data supplied by the British Oceanographic Data Centre (BODC). This procedure provides a more detailed density field very useful to describe the distribution of the meridional density gradient. The spin-up phase consists of a 6 month run using surface climatological momentum fluxes derived from the near surface analyses of the European Centre for Medium-Range Weather Forecasts ECMWF [75]. Surface temperature and salinity are relaxed to climatological data during the spin-up phase. After this period the model is run for 1 year using daily heat, mass and momentum fluxes from the ECWMF large scale forecast model for the year of 1994. The spatial resolution of the ECWMF fluxes was 0.5º by 0.5º. The data is interpolated spatially for the model grid and temporally for the model time step.

The results were compared with available data and previous works concerned with the circulation in the area. The model was able to reproduce the general patterns of the circulation as well as the seasonal variability (Figures 14 and 15 show the velocity fields in winter and summer for the OMEX[1] study area).

The transports were predominantly along slope especially in the OMEX box[2]. However the total amount of water exported from the shelf/slope to the deep ocean along the west coast of Iberia was relatively high (2 to 4 Sv). The exchange seems to have preferential locations since most of the cross-slope transport occurred between 38ºN and 40ºN (the role of the canyons of Nazaré and Setubal is not focused here but it is probably very important and should be subject of detailed studies in the future). This emphasizes the need to look at the OMEX fluxes for the whole Iberian margin, instead of considering only the OMEX box. Finally we should point out that filaments of cold water during the upwelling season might contribute significantly to cross slope exchange. However to generate filaments in the model we need a very high resolution – 2 km. We also need to cover a very large area to obtain a good description of the large-scale circulation and this is not compatible with the resolution needed to simulate filaments.

Two other major findings of this modelling work were: 1) The integrated transport in the upper 1500 m between 10.5ºW and the coast was always poleward for the forcing conditions considered in this study. 2) The transport decreased to the North and the decline seemed very well correlated with topography. This finding seems to be supported by current meter data and by previous studies. Our results indicate that the surface

---

[1] OMEX: Ocean Margin Exchange is a MASTII/III project funded by EU DG Research.

[2] OMEX box is the area off Galicia between 41º 30´N and 43º 30´N and 11ºW.

poleward current over the slope was a permanent feature at least for 1994. However this was a year with low upwelling index in summer months and may be viewed as an anomalous year. It is tempting to state that: 1) the poleward surface current is always there as long as the meridional component of windstress is not strong enough to revert the flow and 2) The reversal of the flow occurs first over the shelf and may not occur over the slope.
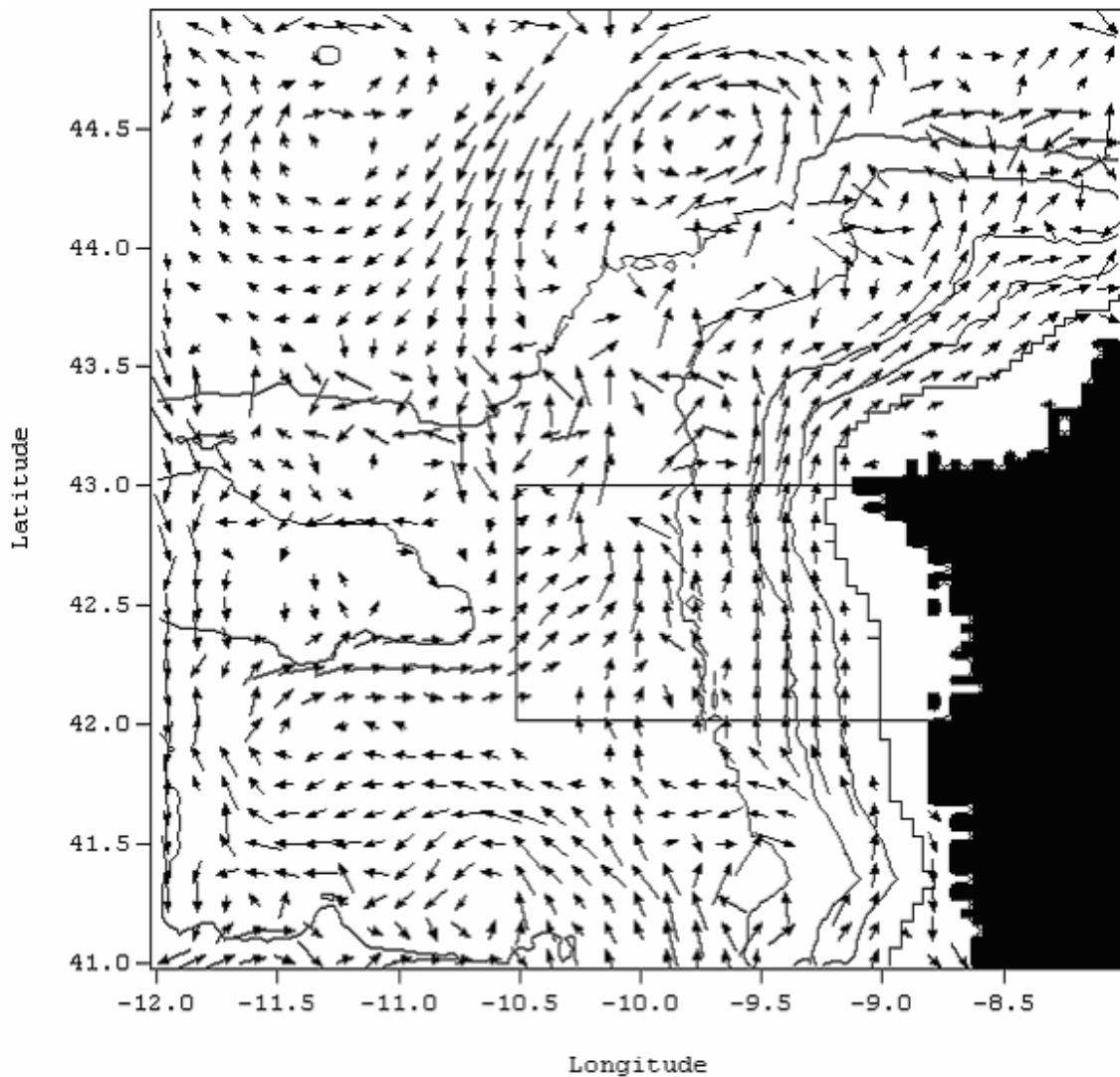
Figure 14 - Velocity field at layer 5 (130 m) on 15 January 1994. Maximum velocity plotted is 30 cm/s and minimum is 2 cm/s. Depth contours represented are for 200 m, 500 m, 1000 m, 2000 m and 3000 m. The overlaid box represents the OMEX box.
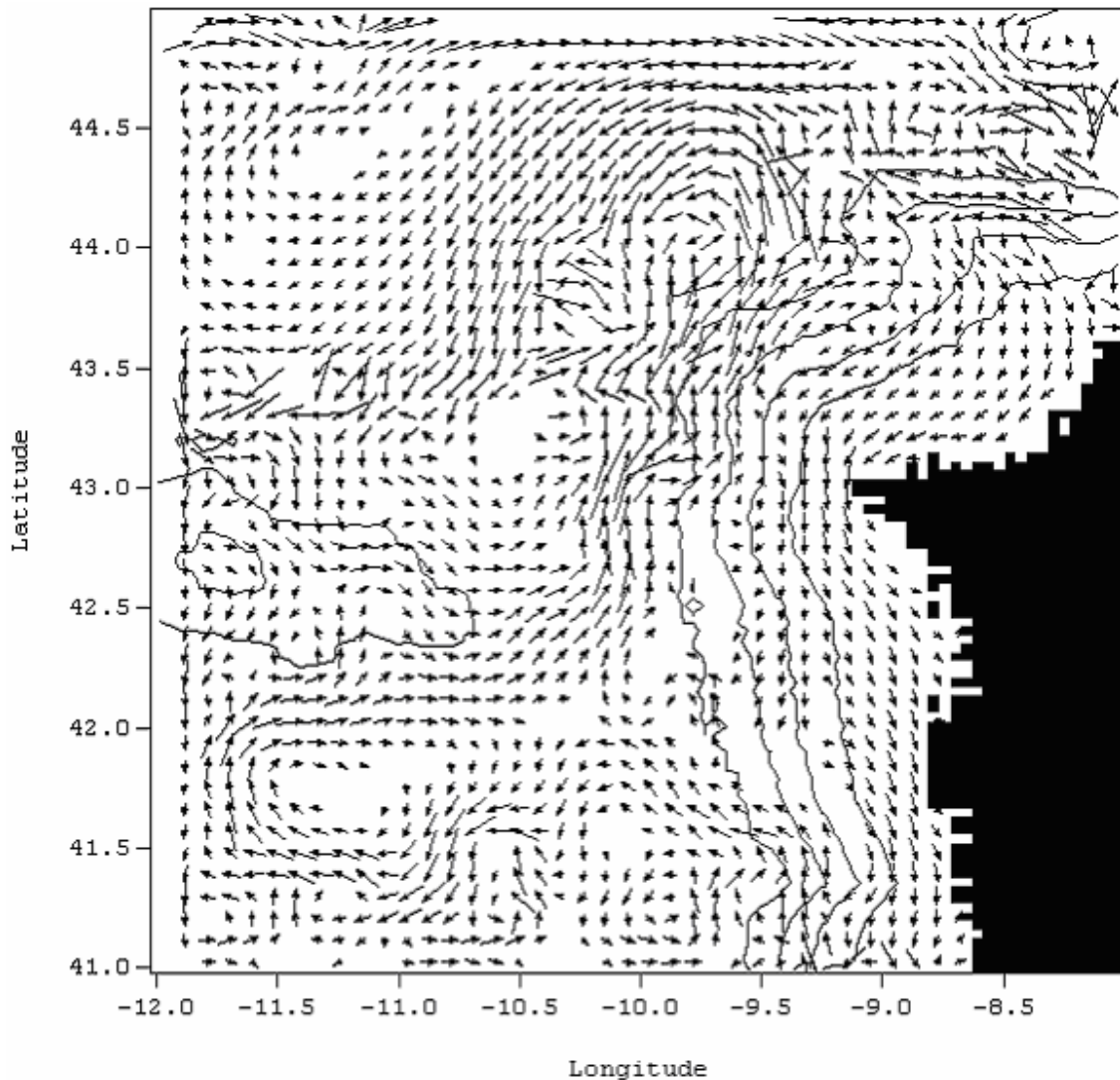
Figure 15 - Velocity field at layer 2 (20 m) on 15 July 1994. Maximum velocity plotted is 20 cm/s and minimum is 2 cm/s. Depth contours represented are for 200 m, 500 m, 1000 m, 2000 m and 3000 m. Note the equatorward jet over the shelf associated with upwelling favourable winds and the poleward flow further offshore.

To have a more realistic description of the circulation and fluxes off Iberian Peninsula we need to improve the horizontal resolution to simulate filaments. Other possible improvements are: 1) to consider river runoff; 2) to use biharmonic diffusion that acts predominantly on submesoscales allowing mesoscale eddy generation and, 3) to consider variable in time conditions at the strait of Gibraltar that might be important to have a better description of variability at MW levels.

Results of sediment transport modelling in the Portuguese Coast

The sediment transport model was used to study the northern Portuguese continental shelf sediment dynamics using one of the most extensive data set available, acquired by the Portuguese Hydrographic Institute. Although the data set is still sparse both in terms of temporal and spatial coverage, model predictions capture the main processes related to shelf sedimentary dynamics. A complete data set can hardly be obtained only experimentally. Coupling this model to a circulation and wave propagation model is certainly the best strategy for future developments.

Currents

Current meter data was acquired in the mid and inner shelf, off Cabo Mondego at depths of 27 m, 37 m and 83 m (see figure 16 and table 1 for details). Current meter time series were filtered with a low-pass Butterworth filter of order 7 and a cut-off period of two hours. Since current meter records were contaminated by surface wave energy, it was subtracted from mean orbital wave velocities computed from the knowledge of the surface wave field. The rectified current velocities are plotted in figure 17. These velocities are typical of shelf velocities, with magnitudes around 10 to 15 cm/s, without any significant difference between the three records. Spectral analysis has shown that tidal motion contains most of the flow variability.

Table 1. Synthesis of current meter data.

Location	Deployment code (figure 16)	Depth (m)	Height from bottom (m)	Sampling interval (min)	Start	End
40°05.1'N 08°56.6'W	A	27	1.0	20	19:00 03/06/82	23:00 30/06/82
40°03.7'N 08°58.5'W	B	37	1.0	20	19:40 02/06/82	10:20 11/08/82
40°13.5'N 09°06.0'W	C	83	1.5	10	15:50 13/04/83	19:40 09/06/83
40°13.5'N 09°06.0'W	C	83	1.5	10	16:20 22/06/83	12:10 30/08/83
40°13.5'N 09°06.0'W	C	83	1.5	20	21:00 30/08/83	03:40 14/09/83
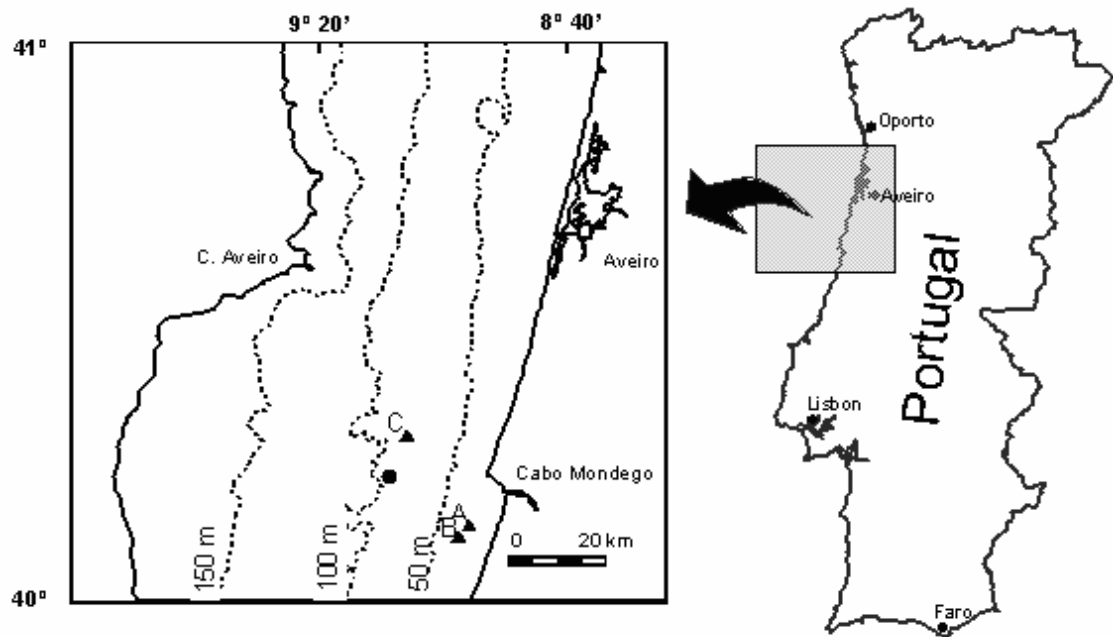
Figure 16 - Current meter deployment sites (solid triangles) and wave-buoy location (solid circle). Dashed lines represent depth contours.
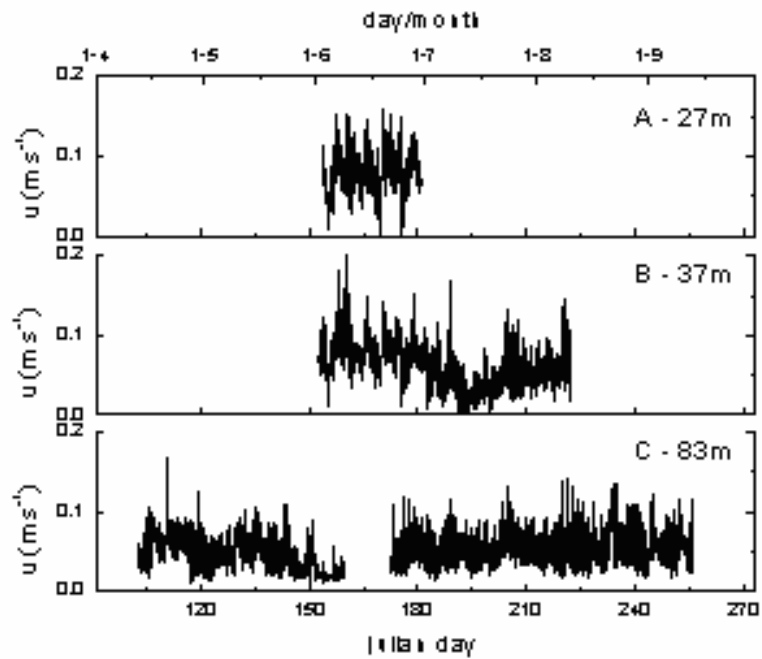
Figure 17 – Current time series.

Waves

Analysed wave data was record by a wave buoy located at a depth of 83 m (figure 16), maintained by the Portuguese Hydrographic Institute (figure 18).
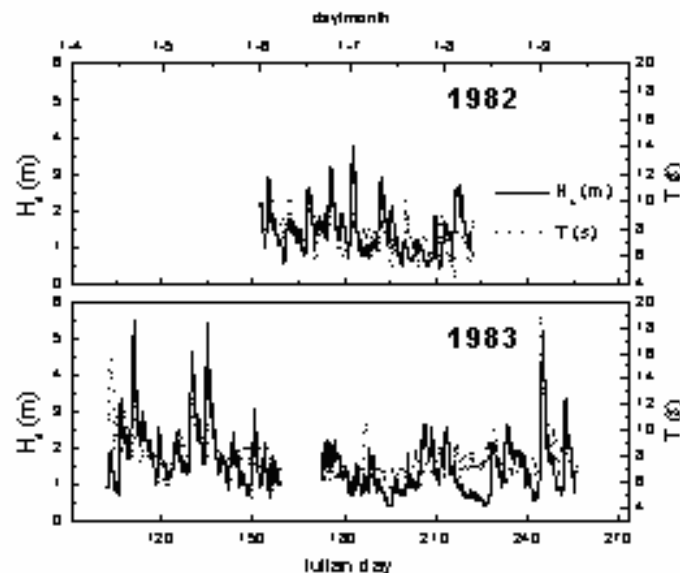
Figure 18. Time series of significant wave height (solid) and wave period (dashed).

In the studied temporal period it is possible to perceive that the "summer" conditions are very well represented while the more energetic conditions, typical of "winter" conditions, are much worse represented. Nevertheless, during the studied period three storms with waves heights greater than 5.0 m were registered.

Sedimentary Cover

The sediment-grain-size used as input into the model represents the median of the two main deposits type identified in the inner and mid shelf: littoral and mid shelf deposits fine sand deposits and mid shelf coarse sedimentary deposits.

Results of sediment transport model

Results confirmed that the Portuguese shelf (at least the mid and inner parts) is clearly wave dominated, with the majority of sediment transport occurring during time of energetic long period waves (figure 20). During the studied time intervals, the waves revealed to be the only mechanism capable of remobilising the sedimentary particles, while the current presented always a reduced intensity, functioning only as a transport mechanism to particles put in suspension by the waves (figure 20).

Moreover, while the major current component is tide related the resulting current related transport has a very weak magnitude. This fact explains the apparent contradiction between the existences of high energetic levels at bottom, with frequent remobilisation

occurrences, and the apparent immobility of the shelf deposits observed by several authors. In fact, as supported by the present observations, as the frequent mobilization is not associated with strong currents, the effective sediment transport is always of reduced intensity, enabling the conservation of deposit identity.
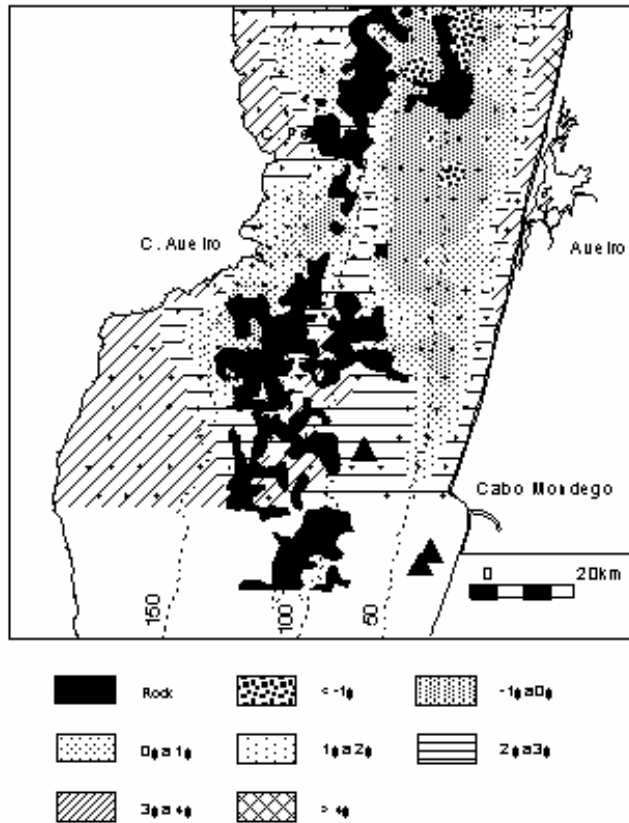
Figure 19 – The superficial sediment distribution (contours in phi) on the northern Portuguese continental shelf. Dashed lines represent depth contours in meters.
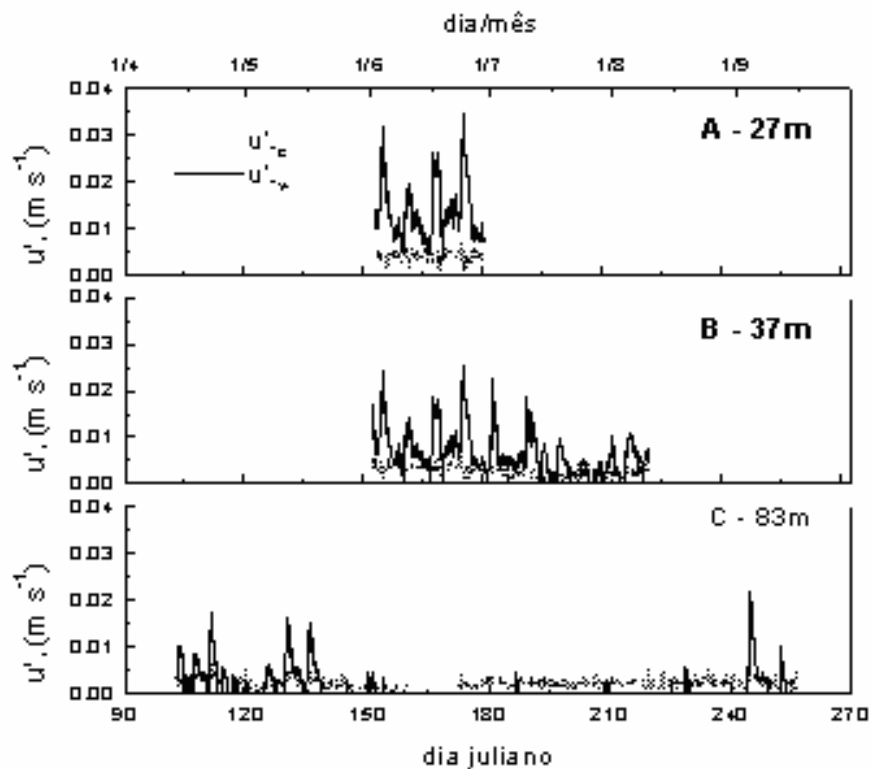
Figure 20 – Comparison between current (u'_{*c} - dashed) and wave (u'_{*w} - solid) related shear velocity computed for a fine sand bottom.

In the middle and outer shelf the modern sedimentation is composed by fine particles (very fine sand or smaller) transported exclusively in suspension, and there is no exchange between median and coarse sand with the inner shelf. The sedimentary transport of the coarse factions of sand is low and essentially related with low frequent and high energetic events. In the middle shelf, the presence of high energetic conditions (wave related) associated with the frequent presence of large bed forms (associated with relict deposits, figure 21) turns this area in a temporary deposition zone. The definitive deposition of fine particles is made in the outer shelf or at greater depths.
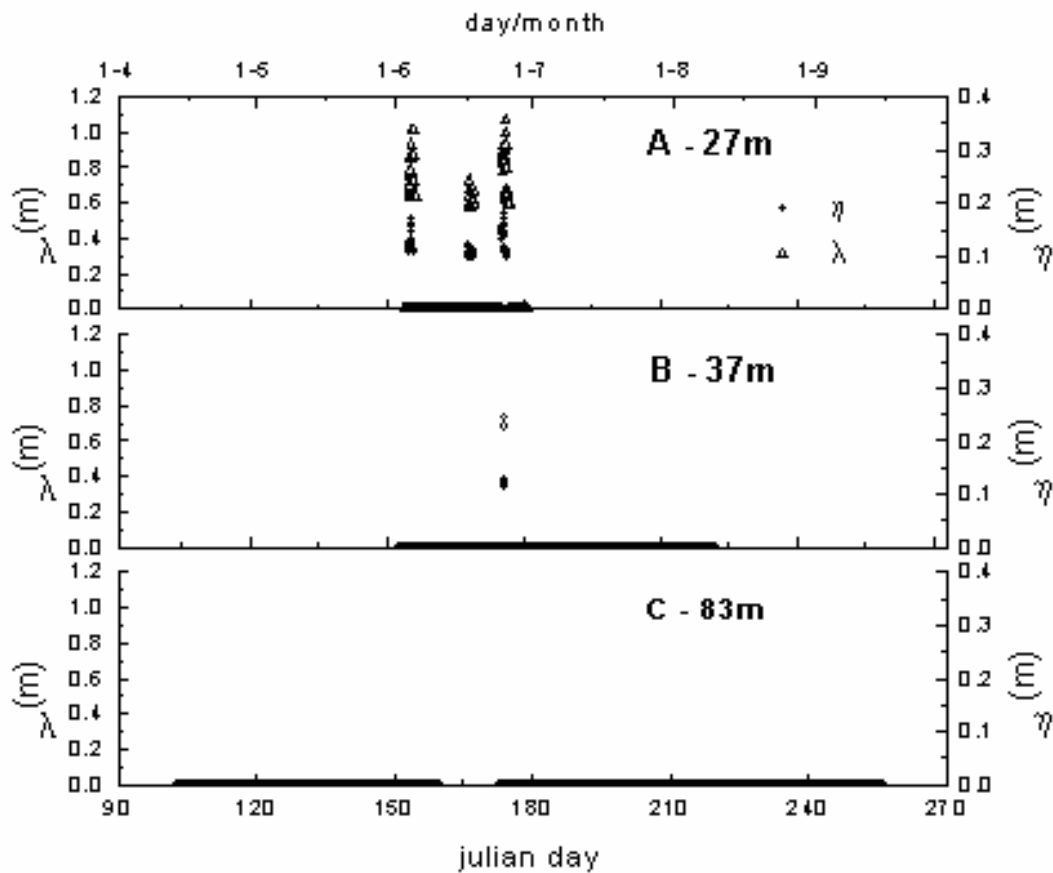
Figure 21 – Computed bedform length and height variation for coarse sand deposits.

Conclusions

Common physical and biogeochemical processes take place in the continental shelf and in estuaries, although the relative importance varies a lot from place to place. In this paper a revision of those processes was done and results were presented for the Portuguese shelf and Tagus estuary using the same computer code. Some basic conditions to obtain a generic model were described.

To achieve a general modelling tool, the model must be able to use the most common vertical coordinates and need to be interdisciplinary. To do so, the model need to be organised in a modular way and be able to accommodate alternative modules, developed by different teams, for each discipline. These features allow its use in areas where the relative importance of physical processes is different and for different purposes (research, management or coastal engineering). This type of tool can generate the critical number of user required to develop supporting software (pre and post processing) required to minimize the time necessary to obtain results.

High biological activity taking place on the shelf and slope is directly related to the supply of nutrients from the deep ocean by vertical movements induced by the slope

current, internal tides and coastal upwelling. In semi-enclosed basins continental discharges and recycling of nutrients are the main support of primary production.

In very shallow areas topography plays a major role for circulation and sigma type coordinates are the most adequate to simulate hydrodynamics. On the contrary, in deeper areas, baroclinic effect scan be as important as topographic and a Cartesian type coordinate is most adequate. An integrated model of the ocean margin must allow more than one type of coordinates.

A model must have a grid as fine as possible to increase accuracy and the number of processes simulated. However increasing the resolution increases the difficulty to analyse results. Time and space integration tools must be developed together with other post-processing tools. Using these tools it was possible to identify the contribution of each part of Tagus estuary for the overall estuary budget of sediments, nutrients and primary producers.

Sediment transport model has shown that the vertical distribution of sediments in the water column is determined mainly by the local physical forcing. To apply this model to the whole shelf a lot of data is required. Coupling of this model to a circulation and wave propagation model will fill gaps of experimental data and will allow the calculation of lateral transport and consequently the calculation of budgets.

Acknowledgements

References

1. Bleck, R., C. Rooth, D. Hu, and L. T. Smith, 1992. Salinity-driven thermocline transients in a wind- and thermohaline-forced isopycnic coordinate model of the North Atlantic. *Journal of Physical Oceanogr*aphy, **22**, 1486-1505.

2. Haidvogel, D. B., J. L. Wilkin and R. Young, 1991. A semi-spectral primitive equation ocean circulation model using vertical sigma and orthogonal curvilinear horizontal coordinates. *Journal of Computational Physics*, **94**, 151-185.

3. Blumberg, A. F. e G. L. Mellor, 1987: A description of a three-dimensional coastal ocean model. Three-Dimensional Coastal Ocean Models, N. Heaps, Ed., Coastal Estuarine Science, Vol. 4, Amer. Geophys. Union, 1-16.

4. Barnard S., B. Barnier, A. Beckman, C. Boening, M. Coulibaty, D. DeCuevas, J. Dengg, C. Dieterich, U. Ernst, P. Herrmann, Y. Jia, P. Killworth, J. Kroeger, M. Lee, C.Le Provost, J-M. Molines, A. New, A. Oschlies, T. Reynauld, L. West and J. Willebrand (September 1997) DYNAMO: Dynamics of North Atlantic Models: Simulation and assimilation with high resolution models. Berichte aus dem Institut fuer Meereskunde an der Christian-Albrechts-Universitat Kiel, **nº 294** 334 pp. ISSN 0341-8561.

5. Santos A. J. P., 1995: Modelo hidrodinâmico de circulação oceânica e estuarina (*in portuguese*). PhD Thesis, IST Lisbon. 273 pp.

6. Martins, F.A., R.J. Neves, P.C. Leitão, 1998. A three-dimensional hydrodynamic model with generic vertical coordinate. *Proceedings of Hidroinformatics98, 2, V. Babovic and L. C. Larsen eds.*, Balkerna/Rotterdam, Copenhague, Denmark, August 1998.1403-1410

7. Martins, F. A., P. C. Leitão, A. Silva and R. Neves, *in press*: 3D modelling of the Sado Estuary using a new generic vertical discretization approach. Accepted for publication in *Oceanologica Acta*.

8. Mellor, G. L., S. Hakkinen, T. Ezer e R. Patchen, 2000: A Generalization of a Sigma Coordinate Ocean Model and an Intercomparison of Model Vertical Grids. Submitted to Ocean Forecasting: Theory and Practice, N. Pinardi (Ed.), Springer-Verlag Publ.

9. Neves , R.J.J., 1985: Étude Expérimentale et Modélisation Mathematique de l'Hydrodynamique de l'Estuaire du Sado. Ph.D Thesis, Université de Liège, Belgium

10. Hervouet J.-M., van Haren L. 1996. Recent advances in numerical methods for fluid flows. Floodplain processes, Anderson MG, Walling DE, Bates PD (eds). Wiley: Chichester; 183-214.

11. Cancino L. and R. J. Neves, 1998: Hydrodynamic and sediment suspension modelling in estuarine systems. part II: Application in the Scheldt and Gironde Estuaries. *Journal of Marine Systems*, **22**, 117-131

12. Portela, L.I., 1996: Mathematical modelling of hydrodynamic processes and water quality in Tagus estuary, Ph.D. thesis, Instituto Sup. Técnico, Tech. Univ. of Lisbon, (in Portuguese)

13. Taboada, J. J., R. Prego, M. Ruiz-Villarreal, M. Gómez-Gesteira, P. Montero, A. P. Santos, V. Pérez-Villar, 1998: Evaluation of the Seasonal Variations in the Residual Circulation in the Ria of Vigo (NW Spain) by means of a 3D baroclinic model. Estuarine, Coastal and Shelf Science.

14. Coelho, H. S., R. J. J. Neves, P. C. Leitão, H. Martins and A. Santos, 1999: The slope current along the Western European Margin: a numerical investigation. *Bol. Inst. Esp. Oceanogr.*, **15**, 61-72.

15. Miranda, R., R. Neves, H. Coelho, H. Martins, P. C. Leitão and A. Santos, 1999: Transport and Mixing Simulation Along the Continental Shelf Edge Using a Lagrangian Approach, *Bol. Inst. Esp. Oceanogr.*, **15**,39-60

16. Phillips N.A., 1957: A coordinate system having some special advantages for numerical forecasting. *J. Meteorol.*, **14**, pp. 184-185.

17. Leendertsee J. J., 1967: Aspects of a Computational Model for Long Water Wave Propagation. *Rand Corporation, Memorandum **RH-5299-RR***, Santa Monica.

18. Gaspar, P.G., Grégoris, Y., Lefevre, J.-M., 1990. A simple eddy kinetic energy model for simulations of the oceanic vertical mixing: tests at station Papa and Long-Term Upper Ocean Study site. Journal of Geophysical Research 95, 16179-16193.

19. Galperin, B., Kantha, L.H., Hassid, S., Rosati, A., 1988. A quasi-equilibrium turbulent energy model for geophysical flows. Journal of the Atmospheric Sciences 45, 55-62.

20. Bougeault, P., Lacarrère. P. 1989. Parameterization of orography-induced turbulence in a meso-beta scale model. Monthly Weather Review 117, 1872-1890.

21. Gargett, A.E., 1984. Vertical eddy diffusivity in the ocean interior. Journal of Marine Research 42, 359-393.

22. Fredsøe, J. and Deigaard, R., 1992: *Mechanics of Coastal Sediment Transport*. Advanced Series on Ocean Engineering, vol. 3, World Scientific, 366 p.

23. Nielsen, P., 1992: *Coastal bottom boundary layer and sediment transport.* Advanced Series on Ocean Engineering, vol. 4, World Scientific, 324 p.

24. Van Rijn, L.C., 1993: *Principles of sediment transport in rivers, estuaries and coastal seas*. Aqua Publications, Amsterdam.

25. Nittrouer, C. and Wright, D., 1994: Transport of particles across continental shelves. *Reviews of Geophysics*, **31**, 85-113.

26. Soulsby, R.L., 1997: *Dynamics of marine sands*. Thomas Telford Publ., London, UK, 249p.

27. Bailard, J.A., 1981: An energetics total load sediment transport model for a plane sloping beach. *Journal of Geophysical Research*, **86**, 10938-10954.

28. Soulsby, R.L.; Hamm, L.; Klopman, G.; Myrhaug, D.: Simons, R.R. and Thomas, G.P. 1993: Wave-current interaction within and outside the bottom boundary layer. *Coastal Engineering*, **21**, 41-69.

29. Smith, J.D., 1977: Modeling of sediment transport on continental shelves. *In: The Sea*, **6**, John Wiley, New York, 539-577.

30. Grant, W.D. and Madsen, O.S., 1979: Combined wave and current interaction with a rough bottom. *Journal of Geophysical Research,* **84**, 1797-1808.

31. Grant, W.D. and Madsen, O.S., 1986: The continental shelf bottom boundary layer. *Annual Review of Fluid Mechanics*, **18**, 265-305.

32. Fredsøe, J., 1984: Turbulent boundary layer in wave-current motion. *Journal of Hydraulic Enginnering,* ASCE, **110**, 1103-1120.

33. Davies, A.G.; Soulsby, R.L. and King, H.L., 1988: A numerical model of the combined wave and current bottom boundary layer. *Journal of Geophysical Research*, **93**, 491-508.

34. Justesen, P.,1988: Prediction of turbulent oscillatory flow over rough beds. *Coastal Engineering*, **12**, 257-284.

35. Nielsen, P., 1981: Dynamics and geometry of wave generated ripples. *Journal of Geophysical Research,* **86**, 6467-6472.

36. Grant, W.D. and Madsen, O.S., 1982: Moveable bed roughness in unsteady oscillatory flow. *Journal of Geophysical Research,* **87**, 469-481.

37. Wiberg, P.L. and Harris, C.K., 1994: Ripple geometry in wave-dominated environments. *Journal of Geophysical Research*, **99**, 775-789.

38. Li, M.Z.; Wright, L.D. and Amos, C.L., 1996: Predicting ripple roughness and resuspension under combined flows in a shoreface environment. *Marine Geology*, **130**, 139-161.

39. Nielsen, P., 1991: Combined convection and diffusion: a new framework for suspended sediment modelling. *Proceedings of Coastal Sediments '91*, ASCE, 418-431.

40. Taborda, R. and Dias, J.A., 2000: Prediction of Wave Related Bedform Geometry. *3º Simpósio sobre a Margem Continental Ibérica Atlântica,* Faro: 257-258.

41. Li, M. Z. and Amos, C. L. 1998. Predicting ripple geometry and bed roughness under combined waves and currents in a continental shelf environment. *Cont. Shelf Research*, **18**: 941-970.

42. Madsen, O. S., 1991: Mechanics of cohesionless sediment transport in coastal waters, *Proceedings of Coastal Sediments '91*, ASCE, 15-27.

43. Glenn, D.A. and Grant, W.D., 1987: A suspended sediment correction for combined wave and current flows. *Journal of Geophysical Research,* **85**, 1797-1808.

44. Deigaard, R., 1991: On the turbulent diffusion coeficient for suspended sediment. *Progress Report nº 73*, Inst. of Hydrodynamics and Hydraulic Engineering, ISVA, Techn. Univ. Denmark, 55-66.

45. Dyer, K.R. and Soulsby R.L., 1988: Sand transport on the continental shelf. *Annual Review of Fluid Mechanics*, **20**, 295-324.

46. Garcia, M. and Parker, G., 1991: Entrainment of bed sediment into suspension. *Journal of Hydraulic Engineering,* **117**, 414-435.

47. Engelund, F. and Fredsøe, J., 1976: A sediment transport model for straight alluvial channels. *Nordic Hydrology* **7**, 293-306.

48. Vincent, C. and Green, M.O., 1990: Field measurements of the suspended sand concentration profiles and fluxes and of the resuspension coefficient γ_0 over a rippled bed. *Journal of Geophysical Research,* **95**, 11591-11601.

49. Dyer, K.R., 1980: Velocity profiles over a rippled bed and the threshold of movement of sand. *Estuarine Coastal Mar. Sci.*, **10**, 181-199.

50. Hill, P.; Nowell, R.M and Jumars, P.A., 1988: Flume evaluation of the relationship between suspended sediment concentration and excess boundary shear stress. *Journal of Geophysical Research,* **92**, 12499-12509.

51. Drake, D.E. and Cacchione, D.A., 1992: Wave-current interaction in the bottom boundary layer during storm and non-storm conditions: observations and model predictions. *Continental Shelf Research*, **12**, 1331-1352.

52. Vincent, C. and Downing, A., 1994: Variability of suspended sand concentrations, transport and eddy diffusity under non-breaking waves on the shoreface. *Continental Shelf Research*, 14, pp. 223-250.

53. Partheniades, E., 1965. Erosion and deposition of cohesive soils. J. Hydr. Div., ASCE, 91, No. HY1 : 105-139.

54. Dyer, K.R., 1986: *Coastal and estuarine dynamics.* Wiley and Sons, Chichester, 342p.

55. Krone, R.B. , 1962. Flume studies of the transport +in estuarine shoaling processes. Hydr. Eng. Lab., Univ. of Berkeley, California, USA.

56. Odd, N.V.M. 1986**.** Mathematical Modelling of Mud transport in Estuaries, Int. Symp. Physical Processes in Estuaries, 9-12 September 1986.

57. Vale, C., Sundby, B., 1987: Suspended sediment fluctuations in the Tagus estuary on semidiurnal and fortnightly time scales, Estuarine, *Coastal Estuarine and Shelf Science*, 27, 495-508.

58. Vale, C., Cortesão, C., Castro, O., Ferreira, A.M., 1983: Suspended-sediment response to pulses in river flow and semidiurnal and fortnightly tidal variations in a mesotidal estuary, *Marine Chemistry*, 43, 21-31.

59. Silva, M.C., Moita, T. & Figueiredo, 1986[a]. Controlo da qualidade da água. Resultados referentes às observações realizadas em 1982 e 1983. Estudo Ambiental do Estuário do Tejo (3°série) n°7. Secretaria de Estado do Ambiente e Recursos Naturais, Lisboa, pp.1-139.

60. Ambar, I. J. 1985. Seis meses de medições de correntes, temperaturas e salinidades na vertente continental Portuguesa a 40° N (*in portuguese*). Grupo de Oceanografia. Universidade de Lisboa. Technical Repport. 1/85: 40 pp. Lisbon

61. Ambar I., A. Fiúza, T. Boyd and R. Frouin, 1986: Observations of a warm oceanic current flowing northward along the coasts of Portugal and Spain during Nov-Dec 1983. *Eos Trans*. AGU, 67(144), 1054

62. Huthnance J. M., 1986: The Rockall slope current and shelf edge processes, *Proc. R. Soc. Edinburgh Sect. B*, **88**, 83-101

63. Frouin R., A. Fiúza, I. Ambar and T. J. Boyd, 1990: Observations of a poleward surface current off the coasts of Portugal and Spain during the winter. *J. Geophys. Res*., **95**, 679-691.

64. Haynes, R. and E. D. Barton ,1990: A poleward flow along the Atlantic coast of the Iberian peninsula, *J. Geophys. Res*., 95, 11425-11141

65. Pingree R. and B. Le Cann, 1989: Celtic and Armorican slope and shelf residual currents. *Prog. Oceanogr*., **23**, 303-338.

66. Lynn, R. J. and J. J. Simpson. 1987. The California current system: The seasonal variability of its physical characteristics. *J. Geophys. Res*. **92**: 12947-12966.

67. Pingree R. and B. Le Cann, 1990: Structure, strength and seasonality of the slope currents in the Bay of Biscay region. *J. Mar. Biol*, **70**, 857-885.

68. McCreary, J. P., P. Kundu and S.Y. Chao. 1987. On the dynamics of the California current system. *J. Mar. Res*. **45**: 1-32.

69. Huthnance J. M., 1984: Slope Currents and "JEBAR". *J. Phys. Oceanog*., 14, 795-810.

70. McCreary, J. P., S. R. Shetye and P. Kundu. 1986. Thermohaline forcing of eastern boundary currents: With application to the circulation off west coast of Australia. *J. Mar. Res*. **44**: 71-92

71. Weaver, A. J. and J. H. Middleton, 1990. An analytic model for the Leeuwin Current off western Australia. *Continental Shelf Research,* **10**: 105-122.

72. Visbeck, M., J. Marshall, T. Haine and M. Spall, 1997: Representation of topography by sahved cells in a height coordinate ocean model. *Mon. Wea. Rev*., **125**, 2293-2315.

73. Levitus, S. and., T. P. Boyer, 1994. World Ocean Atlas 1994. Volume 4: NOAA Atlas NESDIS 4, 117pp.

74. Levitus, S., R. Burgett and T. P. Boyer, 1994. World Ocean Atlas 1994. Volumes 1 and 2: NOAA Atlas NESDIS 3, 99pp.

75. Trenberth, K. E., W. G. Large and J. G. Olsen, 1990: The mean annual cycle in global wind stress. J. Phys. Oceanogr., 20, 1742-1760.